ACS Macro Letters

Letter

pubs.acs.org/macroletters

Metallopolymer-Based Shape Anisotropic Nanoparticles

Bernhard V. K. J. Schmidt,[†,‡,§] Johannes Elbert,[†,∥] Daniel Scheid,[∥] Craig J. Hawker,*[,‡] Daniel Klinger,*[,‡] and Markus Gallei*[,∥]

[‡]Materials Research Laboratory, University of California, Santa Barbara, California 93106, United States

[∥]Ernst-Berl Institute for Chemical Engineering and Macromolecular Science, Technische Universität Darmstadt, Alarich-Weiss Str. 4, 64287 Darmstadt, Germany

Supporting Information

ABSTRACT: The formation of nanostructured shape anisotropic nanoparticles from poly(ferrocenylsilane)-*b*-poly(2-vinylpyridine) (PFS-*b*-P2VP) block copolymers is presented. Ellipsoidal particles with an axially stacked lamellar structure and nanosheets with a hexagonal structure of PFS cylinders are obtained under neutral wetting conditions through the use of a mixed surfactant system during self-assembly. In contrast to traditional systems, the resulting particle structure is strongly influenced by crystallization of the PFS domains under colloidal confinement with lamella-forming PFS-*b*-P2VP block copolymers leading to cylindrical morphologies. A blending approach was developed to control this morphological change and by the addition of PFS homopolymers, ellipsoidal particles with a lamellar structure could also be obtained. Ultimately, the spatial control over two orthogonal functionalities was exploited to demonstrate morphology transitions for nanosheets upon the exposure to methanol as solvent for P2VP and $FeCl_3$ as a redox stimulus, opening up a variety of applications in the field of stimuli-responsive materials.

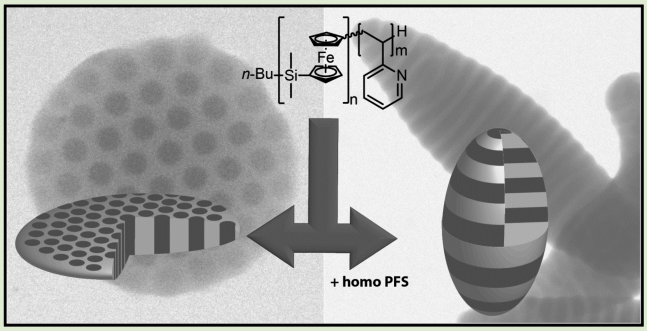

The unique performance of many natural materials is a direct result of the combination of multiple structural features in a synergistic fashion.[1] Highly specific functional properties are achieved by simultaneously controlling shape anisotropy, morphology, and stimuli-responsiveness from the nano- to the micrometer length scale. While this has long inspired researchers to strive for similar abilities in synthetic materials, approaching nature's extraordinary level of control remains a challenge.[2]

One promising approach to such complex materials is based on controlling the self-assembly of block copolymers (BCPs) in nanoparticles upon solvent evaporation from emulsions. In such three-dimensional confinements, phase-separation gives access to unique structures and is dramatically influenced by the particle/water interface. One promising strategy to selectively tune the BCP self-assembly in these colloidal systems is based on using functional surfactants to adjust the surface energies between the different blocks and the surrounding medium. This facile and scalable methodology not only allows control over particle morphology, but also the overall shape.[3−12]

The increasing availability of nanostructured shape anisotropic particles[13,14] is of significant interest as it opens up a variety of applications due to their unique properties, for example, in optics[15] or in cell internalization.[16] Recent examples include convex-shaped nanodiscs/-sheets with cylindrical domains[17,18] (perpendicular to the long axis) and striped ellipsoidal nanoparticles.[6,19] In such systems, both BCP domains are adjoining the particle surface, which enables access by chemical reagents present in the surrounding medium. In the case of stimuli-responsive BCPs, a specific response of a domain can lead to an overall change of the particles' structure. This has recently been demonstrated by the preparation of dynamic shape changing particles that utilize the pH responsiveness of the P2VP domains in a PS-*b*-P2VP block copolymer.[20]

To expand the scope of nanostructured shape anisotropic particles, the self-assembly of block copolymers that are responsive to different (multiple) stimuli was examined using poly(ferrocenylsilane)-based materials. Among the broad variety of stimuli-responsive mechanisms, redox-reactions allow changes in the properties of polymeric materials to be triggered not only by the addition of redox-agents but also by applied electrical potentials.[21] Over the past decade, especially ferrocene-containing polymers[22,23] have been shown to exhibit the unique ability to (electro)chemically switch moieties back and forth between ferrocene and ferrocenium.[21,23−26] Since this oxidation/reduction cycle is accompanied by a transition from a hydrophobic to a hydrophilic state,[27−29] such redox-active polymers have been utilized for a variety of applications, for example, for releasing dyes from redox-responsive nanocapsules,[29−31] for switching the surface wettability and

Received: May 27, 2015
Accepted: June 16, 2015
Published: June 24, 2015

DOI: 10.1021/acsmacrolett.5b00350
ACS Macro Lett. 2015, 4, 731−735

membrane gating,[32−34] for addressing metallopolymer-based colloidal crystals or inverse opal films,[35,36] or for reversible activity modulation of immobilized catalysts.[37] From a morphology viewpoint, block copolymers based on semicrystalline[38] PFS have also attracted significant attention for the preparation of well-defined nanostructures both in the bulk state and in selective solvents by crystallization driven self-assembly (CDSA).[39−45]

Taking advantage of these unique attributes for ferrocene containing polymers, we propose to investigate the particle constrained phase-separation of poly(ferrocenylsilane)-*b*-poly(2-vinylpyridine) (PFS-*b*-P2VP) block copolymers leading to two new types of shape anisotropic nanoparticles: (1) ellipsoidal nanoparticles with an axially stacked lamellar structure and (2) flattened nanosheets (or convex lenses) with a hexagonally packed cylinder structure perpendicular to the long axis. In comparison to previously described systems, these novel PFS-*b*-P2VP particles would ultimately allow a double stimuli-responsive behavior due to the pH responsive P2VP block and the redox responsive PFS block. This approach would therefore dramatically broaden the scope of shape anisotropic nanostructured particles due to the spatial control over two distinctly different responsive chemical functionalities.

Preparation of PFS-based particles was achieved via block copolymer self-assembly upon solvent evaporation from emulsions which were prepared by simple vortexing and ultrasonication (Scheme 1; see SI for experimental details). To selectively access different morphologies, the volume fractions f_{PFS} and f_{P2VP} of the PFS and the P2VP blocks were changed in a systematic manner. While this is known to give control over the bulk morphology, colloidal systems also require controlling the influence of the particle surface and associated interfacial energies as additional structure-directing factors. Here, a common requirement for both targeted structures is the neutral wetting of the BCP/water interphase with both blocks. Following a previously reported procedure for surfactant-controlled self-assembly, a mixture of two surfactants, cetyl trimethylammonium bromide (CTAB) and 16-hydroxy-cetyl triethylammonium bromide (CTEAB−OH), was used to ensure comparable interfacial energies of both blocks with the surrounding medium. Here, CTEAB−OH shows a preference for the P2VP phase due to hydrogen bonding interactions between its hydroxyl group and the P2VP pyridine moieties.[20] In contrast, the unfunctionalized CTAB was assumed to exhibit comparably higher preference for the PFS phase. It has to be mentioned that the pH value for all investigated particle dispersions was in the range of 7 to 8, that is, the 2VP moieties were not affected by protonation which occurs at pH values below 4.9.[46,47]

Following this method, we first examined the synthesis of ellipsoidal particles with a striped lamellar structure by the self-assembly of a symmetric PFS_{60}-*b*-$P2VP_{126}$ diblock copolymer (f_{PFS} = 57 vol %, see SI for synthetic details). As suggested in the literature, it was assumed that the lamellar bulk morphology (Figure 1b) translates to the striped ellipsoidal particle structure under neutral wetting conditions. However, as shown in Figure 1a, particles with the second targeted structure were obtained: a hexagonal assembly of PFS phases with the particles exhibiting a disc-like shape with individual PFS phases as channels through the discs (see also Figure S6). The presence of cylinders running through the full thickness of the disc-like particles was further supported by a series of TEM images with a tilted sample holder (Figure S7) and SEM imaging (Figure 2).

These results clearly indicate that the high surface to volume ratio of nanoparticles can result in BCP morphologies that deviate dramatically from the respective bulk structure. Of perhaps equal significance is the observed hexagonal packing of cylinders perpendicular to the nanosheets' long axis which stems from the neutral wetting of the particle surface by both blocks. This strongly suggests that the BCP/water interphase is not the limiting factor and the necessary requirement for the formation of striped ellipsoidal particles is fulfilled. Following

Scheme 1. Schematic Representation of the Formation of Nanostructured Shape Anisotropic PFS-*b*-P2VP Particles[a]

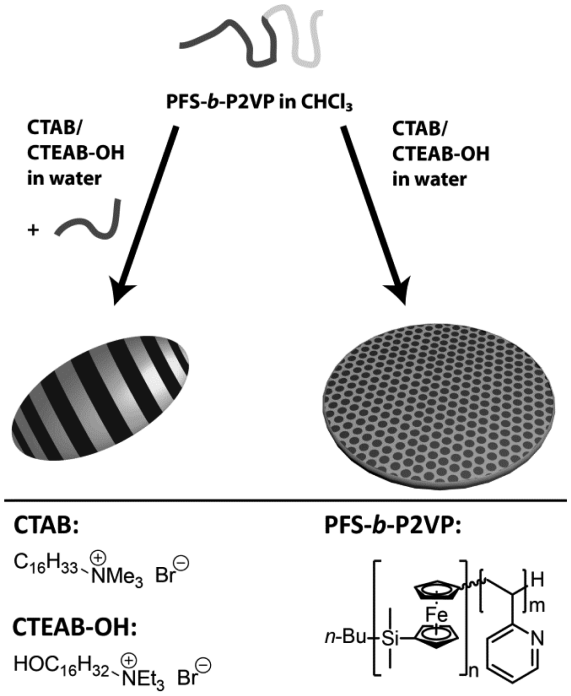

[a]Surfactant mixtures and blending with PFS homopolymer leads to ellipsoid particles with lamella morphology, while assembly of the same diblock copolymer with surfactant mixtures in the absence of homopolymer leads to disk-like particles with cylindrical morphology.

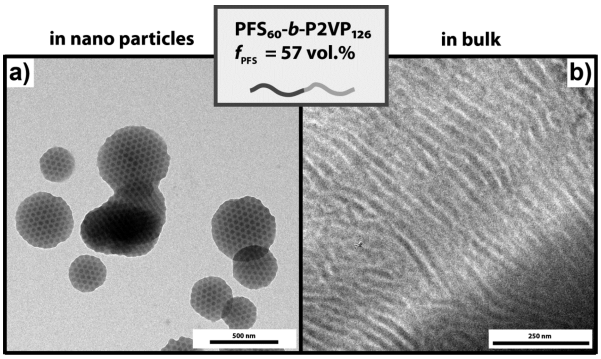

Figure 1. Comparison of PFS_{60}-*b*-$P2VP_{126}$ (f_{PFS} = 57 vol %) morphologies in bulk and under nanoparticle confinement as shown by TEM images. (a) Nanosheets with hexagonally packed cylindrical structures are observed in colloidal confinements under neutral wetting conditions. (b) In contrast, the same BCP exhibits a lamellar bulk morphology.

DOI: 10.1021/acsmacrolett.5b00350
ACS Macro Lett. 2015, 4, 731−735

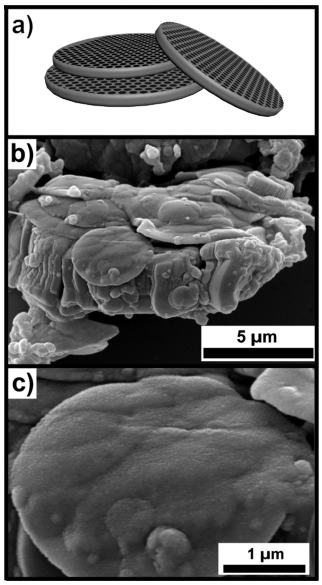

Figure 2. Schematic representation (a) and SEM images of nanosheets formed from PFS_{60}-*b*-$P2VP_{126}$ at different magnifications (b, c).

from these initial results, it was investigated whether BCPs with different block ratios, that is, different bulk morphologies, would give access to the desired ellipsoidal nanoparticles under the same neutral wetting conditions. For this, the volume fraction of PFS in the block copolymer was increased to f_{PFS} = 69 vol % (PFS_{53}-*b*-$P2VP_{58}$) or decreased to 36 vol % (PFS_{55}-*b*-$P2VP_{244}$). Significantly, nanosheets with a hexagonal assembly of the PFS phase were obtained for these polymers as well (see Figure 3a and Supporting Information, Figures S8 and S9) and

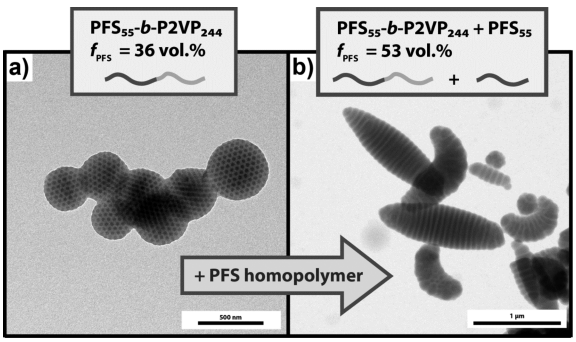

Figure 3. Influence of f_{PFS} and PFS phase composition on the morphology of self-assembled nanoparticles under neutral wetting conditions: (a) nanosheets with a hexagonally packed cylinder structure are obtained from a PFS_{55}-*b*-$P2VP_{244}$ block copolymer. In contrast, blending of the PFS_{55}-*b*-$P2VP_{244}$ block copolymer with 27 wt % of PFS_{55} homopolymer gives striped ellipsoidal particles (b).

only for the extreme case of a PFS volume fraction of 90 vol % (PFS_{53}-*b*-$P2VP_{11}$) did the morphology change to spherical particles with a radial lamellar morphology (Figure S8). As a consequence, the hexagonal morphologies are formed in a large part of the phase diagram from approximately f_{PFS} = 30 vol % to approximately 70 vol % (Table S2). This is in direct contrast to reported systems where nanosheet particles with hexagonal morphologies are typically only formed from block copolymers with volume fractions that directly correspond to a hexagonal morphology in the bulk state.[38]

This unexpected behavior strongly suggests that in these systems, the obtained morphology is not only dependent on the volume fractions of the blocks and the interfacial interactions but also on the semicrystalline nature of the PFS block. As has been elegantly reported by Manners, the crystallization behavior of PFS can overcome the influence of the block copolymer ratio in the formation of specific morphologies via self-assembly.[40] An effect that is especially pronounced in the confinements of nanostructures.[48] To further investigate this effect and to access ellipsoidal particles with a stacked lamellae structure, the influence of the PFS crystallization in the PFS-P2VP system was further tuned. Interestingly, Manners and co-workers recently showed that cocrystallization in PFS-based block copolymer/homopolymer blends significantly shifts the structure of formed nano-objects from fibers to platelets.[49] Based on these considerations, we investigated blends of the cylinder forming diblock copolymer, PFS_{55}-*b*-$P2VP_{244}$, with additional homo PFS_{55}. Blending of the diblock with 27 wt % of the homopolymer leads to an overall PFS volume fraction of f_{PFS} = 53 vol %, which corresponds again to a lamellar bulk morphology with particle formation performed under similar neutral wetting conditions (i.e. 50/50 ratio of CTAB and CTEAB−OH). Interestingly, from this approach ellipsoidal nanoparticles in the size range of 100 nm to 1 μm were obtained exclusively (see Figures 3b and S10). This is in agreement with bulk samples of pure PFS-*b*-P2VP block copolymer, which show a clear lamellar structure for equal volume fractions of both blocks.

Noticeably, for the two systems that both contain a PFS volume fraction of f_{PFS} = 50 vol % (corresponding to a lamellar *bulk* morphology), the morphology of the particle clearly depends on the composition of the PFS phase.

If the PFS domains solely consist of the respective blocks of a symmetrical PFS-*b*-P2VP block copolymer, hexagonally packed cylinder morphologies are observed in flattened nanosheets. In direct contrast, if the PFS domains consist of a mixture of a PFS homopolymer and PFS blocks from a PFS-*b*-P2VP block copolymer, lamellar structures are observed in ellipsoidal particles.

In examining these results, for the pure PFS_{55}-*b*-$P2VP_{244}$ diblock copolymer, the deviation of the cylindrical particle morphology from the lamellar bulk structure suggests a strong influence of PFS crystallization due to colloidal confinement. It is assumed that this can also be attributed to the comparably large volume (64%) of the noncrystalline P2VP chains. In contrast to the densely packed crystalline PFS domains, the P2VP "corona" still exhibits a significant entropic chain repulsion (even though the self-assembly does not occur in solution).[49] In the spatial confinement of nanoparticles, this effect shifts the morphology to the observed cylindrical structure. In the case of PFS/PFS-*b*-P2VP blends, the crystallization process is changed by the addition of PFS homopolymer and assuming that under confinement, the crystallization is initiated by homogeneous nucleation of the homopolymer, the resulting seeds most likely serve as nucleation point for the crystallization of PFS-based block copolymers. In analogy to the work presented by Manners, Winnik and co-workers,[49] it is suggested that the cocrystallization with PFS-*b*-P2VP (in the wet brush regime) increases the spacing between the anchor points of the corona chains. In combination with the colloidal confinement, the resulting decreased "corona" chain repulsion enables the formation of the observed ellipsoidal particles with axially stacked lamellae.

DOI: 10.1021/acsmacrolett.5b00350
ACS Macro Lett. 2015, 4, 731−735

As a result, the self-assembly of PFS-*b*-P2VP metallopolymers under colloidal confinement is controlled by a combination of neutral wetting of the BCP/water interphase through functional surfactants and by tuning the crystallization of the PFS block via blending with the corresponding PFS homopolymer. As shown in the phase diagram in Figure 4, this approach allows facile access to different shape anisotropic particles with very distinct morphologies.

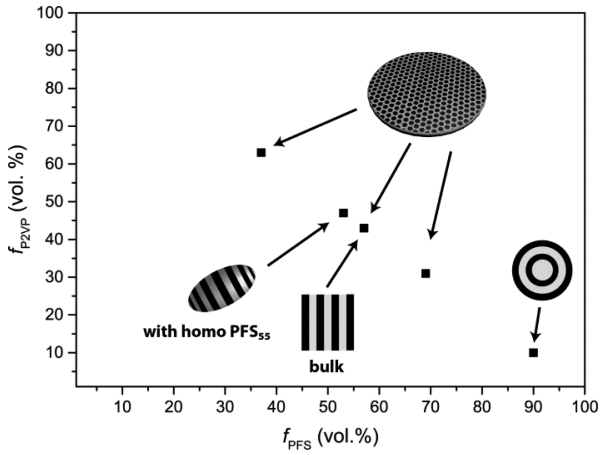

Figure 4. Schematic phase diagram of PFS-*b*-P2VP nanoparticles obtained via solvent evaporation driven block copolymer self-assembly.

The striped ellipsoidal particles and the nanosheets containing hexagonally packed cylinders represent interesting materials due to the orthogonal chemical functionalities of the two polymer phases. In combination with the accessibility of both domains to reagents/stimuli from the surrounding medium, these particles show potential as double responsive materials. To demonstrate the latent multi functionality of these colloidal systems, initial experiments were performed to selectively address each domain. For this we focused on the nanosheets as a model system.

First, the influence of a selective solvent for the P2VP block was probed. The utilization of methanol led to the solvation of the P2VP domains which resulted in a pronounced morphology change from nanosheets with multiple PFS domains to individual PFS-based nanoparticles (Figure 5; for more details, refer to Figure S11) that are assumed to consist of a PFS core with a P2VP corona. Remarkably, the well-defined size of the PFS domains in the hexagonal array of the nanosheets transfers to a very narrow size distribution of the resulting PFS centered nanoparticles. The redox-responsive character of the PFS domains and the associated polarity change from hydrophobic to hydrophilic on oxidation was then investigated. Significantly, addition of an oxidant, $FeCl_3$, to the nanosheets led to changes in the observed particle structures with TEM images of dispersions after treatment with $FeCl_3$ showing the disintegration of the initial particle shapes (Figure S12) due to the increased hydrophilicity of the oxidized ferrocene units. The observed morphology change depicts a transition from well-defined hexagonal arrays of PFS phases in the nanosheets to amorphous nanosized objects as well as worm-like PFS phases. While this clearly indicates the potential of redox-agents to trigger irreversible morphology changes in the PFS-*b*-P2VP nanosheets upon oxidation, the properties of the formed aggregates and the underlying transition mechanism will be subject to future investigations. Ultimately, the formed

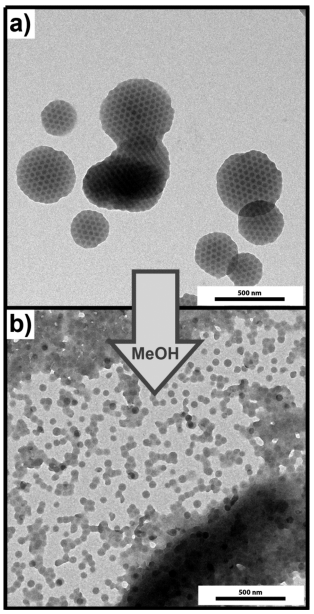

Figure 5. Morphology transition of PFS_{60}-*b*-$P2VP_{126}$ nanoparticles upon addition of methanol as selective solvent for the P2VP domains. Nanosheets with a hexagonally PFS cylinders (a) undergo transformation to PFS-based nanoparticles with a narrow size distribution (b).

structures represent an interesting starting point for further investigations on CDSA by using these in situ generated building blocks.[39,44]

In conclusion, a facile and scalable method for the preparation of novel shape anisotropic nanoparticles formed from PFS-*b*-P2VP metal-containing block copolymers was developed. Control over shape and morphology could be achieved by adjusting the wetting of the BCP/water interphase through functional surfactants and by tuning the crystallization of the PFS domains via blending with respective homopolymers. Unique materials with controlled shape and nanoscale morphology such as ellipsoidal nanoparticles with axially stacked lamellar morphology or nanosheets with hexagonally packed PFS cylinders could be obtained. Ultimately, spatial control over the two orthogonal functionalities present in the PFS-*b*-P2VP diblock copolymers was exploited to demonstrate morphology transitions on exposure to selective solvents and stimuli-responsive shape changes on treatment with redox agents such as $FeCl_3$. The facile control over shape, morphology, and chemical functionality allows these particles to be a powerful generic platform for further studies and applications.

■ ASSOCIATED CONTENT

Supporting Information

Experimental details and further characterization data. The Supporting Information is available free of charge on the ACS Publications website at DOI: 10.1021/acsmacrolett.5b00350.

■ AUTHOR INFORMATION

Corresponding Authors

*E-mail: hawker@mrl.ucsb.edu.
*E-mail: klinger@mrl.ucsb.edu.
*E-mail: m.gallei@mc.tu-darmstadt.de.

DOI: 10.1021/acsmacrolett.5b00350
ACS Macro Lett. 2015, 4, 731−735

Present Address

[§]Max Planck Institute of Colloids and Interfaces, 14424 Potsdam, Germany (B.V.K.J.S.).

Author Contributions

[†]These authors contributed equally (B.V.K.J.S. and J.E.).

Notes

The authors declare no competing financial interest.

■ ACKNOWLEDGMENTS

This work was supported by the MRSEC Program of the National Science Foundation (NSF) under Award DMR-1121053 (C.J.H.), the Institute for Collaborative Biotechnologies through Grant W911NF-09-0001 from the U.S. Army Research Office (B.V.K.J.S., D.K., and C.J.H.). Facilities support from the CNSI-MRL Center for Scientific Computing (DMR-1121053 and CNS-0960316) is acknowledged. The content of the information does not necessarily reflect the position or the policy of the U.S. Government and no official endorsement should be inferred. M.G. and J.E. would like to thank the Landesoffensive zur Entwicklung Wissenschaftlich-ökonomischer Exzellenz (LOEWE "Soft Control"). Support in performing the SEC analyses given by Marion Trautmann and Dr. Matthias Wittemann is gratefully acknowledged. B.V.K.J.S. was supported by a fellowship within the Postdoc-Program of the German Academic Exchange Service (DAAD).

■ REFERENCES

(1) Liu, K.; Jiang, L. *Nano Today* **2011**, *6*, 155.
(2) Sanchez, C.; Arribart, H.; Giraud Guille, M. M. *Nat. Mater.* **2005**, *4*, 277.
(3) Okubo, M.; Saito, N.; Takekoh, R.; Kobayashi, H. *Polymer* **2005**, *46*, 1151.
(4) Jeon, S.-J.; Yi, G.-R.; Yang, S.-M. *Adv. Mater.* **2008**, *20*, 4103.
(5) Kitayama, Y.; Yorizane, M.; Kagawa, Y.; Minami, H.; Zetterlund, P. B.; Okubo, M. *Polymer* **2009**, *50*, 3182.
(6) Jeon, S.-J.; Yi, G.-R.; Koo, C. M.; Yang, S.-M. *Macromolecules* **2007**, *40*, 8430.
(7) Li, L.; Matsunaga, K.; Zhu, J.; Higuchi, T.; Yabu, H.; Shimomura, M.; Jinnai, H.; Hayward, R. C.; Russell, T. P. *Macromolecules* **2010**, *43*, 7807.
(8) Shim, J. W.; Kim, S.-H.; Jeon, S.-J.; Yang, S.-M.; Yi, G.-R. *Chem. Mater.* **2010**, *22*, 5593.
(9) Higuchi, T.; Motoyoshi, K.; Sugimori, H.; Jinnai, H.; Yabu, H.; Shimomura, M. *Macromol. Rapid Commun.* **2010**, *31*, 1773.
(10) Staff, R. H.; Rupper, P.; Lieberwirth, I.; Landfester, K.; Crespy, D. *Soft Matter* **2011**, *7*, 10219.
(11) Kim, B. J.; Bang, J.; Hawker, C. J.; Chiu, J. J.; Pine, D. J.; Jang, S. G.; Yang, S.-M.; Kramer, E. J. *Langmuir* **2007**, *23*, 12693.
(12) Kim, B. J.; Fredrickson, G. H.; Hawker, C. J.; Kramer, E. J. *Langmuir* **2007**, *23*, 7804.
(13) Higuchi, T.; Tajima, A.; Motoyoshi, K.; Yabu, H.; Shimomura, M. *Angew. Chem., Int. Ed.* **2009**, *48*, 5125.
(14) Wyman, I.; Njikang, G.; Liu, G. *Prog. Polym. Sci.* **2011**, *36*, 1152.
(15) Fernández-Nieves, A.; Cristobal, G.; Garcés-Chávez, V.; Spalding, G. C.; Dholakia, K.; Weitz, D. A. *Adv. Mater.* **2005**, *17*, 680.
(16) Champion, J. A.; Mitragotri, S. *Proc. Natl. Acad. Sci. U.S.A.* **2006**, *103*, 4930.
(17) Ku, K. H.; Shin, J. M.; Kim, M. P.; Lee, C.-H.; Seo, M.-K.; Yi, G.-R.; Jang, S. G.; Kim, B. J. *J. Am. Chem. Soc.* **2014**, *136*, 9982−9989.
(18) Ku, K. H.; Yang, H.; Shin, J. M.; Kim, B. J. *J. Polym. Sci. A: Polym. Chem.* **2015**, *53*, 192−199.
(19) Jang, S. G.; Audus, D. J.; Klinger, D.; Krogstad, D. V.; Kim, B. J.; Cameron, A.; Kim, S.-W.; Delaney, K. T.; Hur, S.-M.; Killops, K. L.; Fredrickson, G. H.; Kramer, E. J.; Hawker, C. J. *J. Am. Chem. Soc.* **2013**, *135*, 6649.
(20) Klinger, D.; Wang, C. X.; Connal, L. A.; Audus, D. J.; Jang, S. G.; Kraemer, S.; Killops, K. L.; Fredrickson, G. H.; Kramer, E. J.; Hawker, C. J. *Angew. Chem., Int. Ed.* **2014**, *53*, 7018.
(21) Zhou, J.; Whittell, G. R.; Manners, I. *Macromolecules* **2014**, *47*, 3529−3543.
(22) Whittell, G. R.; Manners, I. *Adv. Mater.* **2007**, *19*, 3439.
(23) Whittell, G. R.; Hager, M. D.; Schubert, U. S.; Manners, I. *Nat. Mater.* **2011**, *10*, 176.
(24) Abd-El-Aziz, A. S.; Agatemor, C.; Etkin, N. *Macromol. Rapid Commun.* **2014**, *35*, 513.
(25) Gallei, M. *Macromol. Chem. Phys.* **2014**, *215*, 699.
(26) Schmidt, B. V. K. J.; Elbert, J.; Barner-Kowollik, C.; Gallei, M. *Macromol. Rapid Commun.* **2014**, *35*, 708.
(27) Giannotti, M. I.; Lv, H.; Ma, Y.; Steenvoorden, M. P.; Overweg, A. R.; Roerdink, M.; Hempenius, M. A.; Vancso, G. J. *J. Inorg. Organomet. Polym. Mater.* **2005**, *15*, 527.
(28) Ma, Y.; Dong, W.-F.; Hempenius, M. A.; Möhwald, H.; Vancso, G. J. *Nat. Mater.* **2006**, *5*, 724.
(29) Hempenius, M. A.; Cirmi, C.; Savio, F. L.; Song, J.; Vancso, G. J. *Macromol. Rapid Commun.* **2010**, *31*, 772.
(30) Staff, R. H.; Gallei, M.; Landfester, K.; Crespy, D. *Macromolecules* **2014**, *47*, 4876.
(31) Staff, R. H.; Gallei, M.; Mazurowski, M.; Rehahn, M.; Berger, R.; Landfester, K.; Crespy, D. *ACS Nano* **2012**, *6*, 9042.
(32) Elbert, J.; Gallei, M.; Rüttiger, C.; Brunsen, A.; Didzoleit, H.; Stühn, B.; Rehahn, M. *Organometallics* **2013**, *32*, 5873.
(33) Elbert, J.; Krohm, F.; Rüttiger, C.; Kienle, S.; Didzoleit, H.; Balzer, B. N.; Hugel, T.; Stühn, B.; Gallei, M.; Brunsen, A. *Adv. Funct. Mater.* **2014**, *24*, 1591.
(34) Zhang, K.; Feng, X.; Sui, X.; Hempenius, M. A.; Vancso, G. J. *Angew. Chem., Int. Ed.* **2014**, *53*, 13789.
(35) Puzzo, D. P.; Arsenault, A. C.; Manners, I.; Ozin, G. A. *Angew. Chem., Int. Ed.* **2009**, *48*, 943.
(36) Scheid, D.; Lederle, C.; Vowinkel, S.; Schäfer, C. G.; Stühn, B.; Gallei, M. *J. Mater. Chem. C* **2014**, *2*, 2583.
(37) Elbert, J.; Mersini, J.; Vilbrandt, N.; Lederle, C.; Kraska, M.; Gallei, M.; Stühn, B.; Plenio, H.; Rehahn, M. *Macromolecules* **2013**, *46*, 4255.
(38) Papkov, V. S.; Gerasimov, M. V.; Dubovik, I. I.; Sharma, S.; Dementiev, V. V.; Pannell, K. H. *Macromolecules* **2000**, *33*, 7107.
(39) Bellas, V.; Rehahn, M. *Angew. Chem., Int. Ed.* **2007**, *46*, 5082.
(40) Mohd Yusoff, S. F.; Hsiao, M.-S.; Schacher, F. H.; Winnik, M. A.; Manners, I. *Macromolecules* **2012**, *45*, 3883.
(41) Qian, J.; Lu, Y.; Chia, A.; Zhang, M.; Rupar, P. A.; Gunari, N.; C.Walker, G.; Cambridge, G.; He, F.; Guerin, G.; Manners, I.; Winnik, M. A. *ACS Nano* **2013**, *7*, 3754.
(42) Qiu, H.; Du, V. A.; Winnik, M. A.; Manners, I. *J. Am. Chem. Soc.* **2013**, *135*, 17739.
(43) Hsiao, M.-S.; Yusoff, S. F. M.; Winnik, M. A.; Manners, I. *Macromolecules* **2014**, *47*, 2361.
(44) Hudson, Z. M.; Boott, C. E.; Robinson, M. E.; Rupar, P. A.; Winnik, M. A.; Manners, I. *Nat. Chem.* **2014**, *6*, 893.
(45) Qiu, H.; Hudson, Z. M.; Winnik, M. A.; Manners, I. *Science* **2015**, *347*, 1329.
(46) Borchert, U.; Lipprandt, U.; Bilang, M.; Kimpfler, A.; Rank, A.; Peschka-Süss, R.; Schubert, R.; Lindner, P.; Förster, S. *Langmuir* **2006**, *22*, 5843.
(47) Kraska, M.; Gallei, M.; Stühn, B.; Rehahn, M. *Langmuir* **2013**, *29*, 8284.
(48) Arsenault, A. C.; Rider, D. A.; Tétreault, N.; Chen, J. I. L.; Coombs, N.; Ozin, G. A.; Manners, I. *J. Am. Chem. Soc.* **2005**, *127*, 9954.
(49) Cambridge, G.; Gonzalez-Alvarez, M. J.; Guerin, G.; Manners, I.; Winnik, M. A. *Macromolecules* **2015**, *48*, 707.

DOI: 10.1021/acsmacrolett.5b00350
ACS Macro Lett. 2015, 4, 731−735